

# Chapter 20

## Performance Evaluation of an Inland Pusher

M. Godjevac and M. Drijver

**Abstract** In order to meet the future exhaust gas emission standards on European inland waterways, ship owners are facing challenges when selecting the optimal power configuration and/or retrofit option. While there are many variations of power configurations for an inland vessel, a typical ship owner is not certain which of those possibilities is the best one. To help tackling these challenges, a comprehensive study has been carried out where various power configurations have been evaluated against the operational profile of an inland pusher on river Rhine. The operational profile was obtained by measuring the fuel rack position and ship speed during the period of 6 months. Comparing the transport efficiency (i.e., fuel consumed versus cargo transported) with the recorded water levels it was shown that the transport efficiency doubles in deep water periods. Furthermore, it was argued that a more flexible power configuration, with an additional shaft line, could contribute to the total efficiency. Based on the operational profile, seven alternative power configurations have been selected. They include: diesel-direct, diesel-electric, gas engine-electric, and a combination of diesel-direct and diesel-electric. Afterwards, an estimate of the total exhaust emissions during one typical voyage was made for all alternative configurations using dynamic models. For the investigated vessel, the diesel direct configuration still is the most efficient configuration regarding the energy consumption. However, regarding NO<sub>x</sub> and PM the performance of power configurations based on gas engines is superior. As an alternative for NO<sub>x</sub> reduction, the effect of SCR installation was also considered which appears to be practical solution for retrofitting as well.

---

M. Godjevac (✉)  
Delft University of Technology, Delft, The Netherlands  
e-mail: [M.Godjevac@tudelft.nl](mailto:M.Godjevac@tudelft.nl)

M. Drijver  
CIG Maritime Technology, Groningen, The Netherlands  
e-mail: [drijvermichiel@gmail.com](mailto:drijvermichiel@gmail.com)

## 20.1 Introduction

Merchant vessels on European inland waterways are typically around 20 years old and owned by small (family) companies. At the same time, exhaust emission regulations on European inland waterways are becoming more stringent. For a ship owner, this situation raises multiple questions regarding the possible power configurations of inland ships and how to meet the future regulations. In order to tackle this issue, a research project under the title “Modernization of Vessels of Inland Waterway Freight Transport” (MoVeIT) is running within the European seventh framework program. This chapter presents some outcomes of the MoVeIT project, as well as the investigation presented in [5], and its main focus point is the optimization of the ship’s drive and power system in such a way that it is matched to the conditions that the ship will face throughout its life. Questions related to the selection of the fuel type (diesel or natural gas), power transmission (direct or electric), and power generation (number and sizes of engines) are answered in this study with respect to their related exhaust emissions and fuel consumptions. An inland pusher operating on the river Rhine is selected as the case study for this investigation. Firstly, the operational profile measurements are done during 6 months sailing period. Also, emission test cycle measurements are done on board of the vessel. Secondly, a selection of alternative power configurations is made, including: diesel-direct, diesel-electric, gas-electric, and hybrid power configurations. Thirdly, dynamic models of all power configurations are created in the Matlab/Simulink environment. Finally, combining the models with the results of the measurements, the total emissions and fuel consumptions are calculated for each power configuration for one typical journey. Figure 20.1 depicts the process that has been used in this investigation.

In total 2 sets of measurements are used in this study and their results are presented in this document. Further, 10 dynamic models of different power configurations are created to estimate their exhaust emissions ( $\text{NO}_x$ ,  $\text{SO}_x$ ,  $\text{CO}_x$ , HC, PM). For diesel direct power configurations, a selective catalyst reduction (SCR) is an option to reduce the  $\text{NO}_x$  emission. The effect of an SCR installation is also considered in this chapter and its urea consumption is calculated as well.

While the title of this book is “Transport of Water Versus Transport Over Water”, the focus of this chapter is rather on the transport over water. Here the performance of an inland pusher is analyzed in terms of its exhaust emissions and



Fig. 20.1 Schematic illustration of the research process



**Fig. 20.2** Veerhaven X in four barges configuration

fuel consumption during operation. However, the fuel consumption and transport efficiency are closely related to the conditions on the river, namely to the water depth, and the scope of this chapter is actually broader than just the transport over water. As shown in this chapter, the transport efficiency drops significantly during periods of low water due to part load conditions in which the pusher is operating. If the level of water could be somehow increased during periods of low water, for example by the transport of water, then the transport over water would be improved as well, and this illustrates how the transport over water may be affected by the transport of water.

An inland pusher called Veerhaven X (see Fig. 20.2) is selected for the case study. This is one of the biggest pushers operating on the river Rhine and it is considered as state of the art amongst inland pushers. The ship operates mostly between Rotterdam and Duisburg pushing the barges with coal and iron upstream from Rotterdam to Duisburg in 4 or 6 barges configuration, depending on the water level and cargo loaded. After leaving its cargo, the ship picks up the empty barges and goes back downstream to Rotterdam. A typical trip takes about 40 h where an upstream voyage is about 24 h and a downstream voyage is about 12 h.

Figure 20.3 shows the power configuration of Veerhaven X. The ship is equipped with three identical mechanically driven diesel direct propulsion trains and four generator sets for auxiliary power. The total installed propulsion power is 4,080 kW. Each propulsion train is equipped with a fixed pitch propeller with 5 blades and 2.05 m diameter.

This chapter is structured according to the research process illustrated in Fig. 20.1. The results of the long-term measurements conducted on-board of Veerhaven X are presented in Sect. 20.2. These measurements define the operational profile of Veerhaven X. Section 20.2 also presents the transport efficiency of the vessel during the period of the operational profile measurements and in Sect. 20.3 the results of exhaust emission measurements are given. In Sect. 20.4,

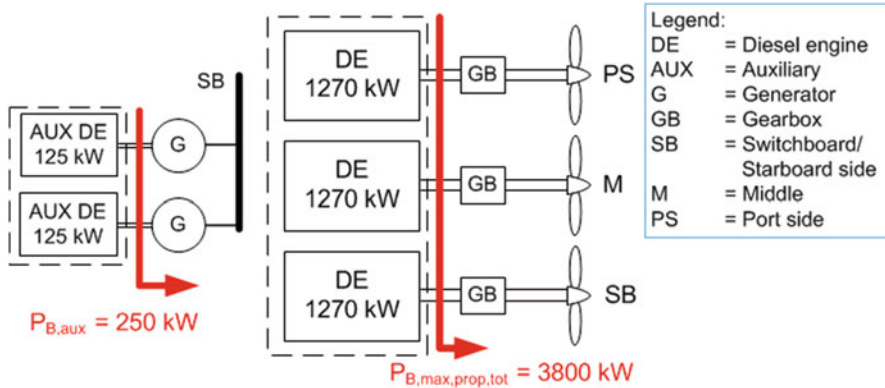


Fig. 20.3 Power configuration of Veerhaven X

alternative power configurations are defined using the operational profile measurements from Sect. 20.2. Subsequently, dynamic models of the selected alternative power configurations are described in Sect. 20.5. The results of the exhaust emission measurements from Sect. 20.3 are then used to calibrate the models in Sect. 20.5. After which the resulting emissions and fuel consumptions from the models of the alternative power configurations are presented in Sect. 20.6. The analysis of the results is given in Sect. 20.7 and the conclusions are presented in Sect. 20.8.

## 20.2 Operational Profile and Transport Efficiency

To get more insight in the long term performance of the ship and its fuel consumption, the operation of the ship is observed during 6 months by measuring the following parameters:

- Fuel rack position of the starboard, middle, and portside engine
- GPS position and speed over ground

In order to get the operational profile of the vessel (i.e., power versus time) it is necessary to calibrate and convert the measurements of the fuel rack position to the power consumption. The fuel rack position is first converted to the fuel flow, which is then converted to the engine power. Figure 20.4 shows the operational profile of the ship and water level recorded during the measurements. According to its mission profile, the operational profile of Veerhaven X is divided in three operational modes: upstream, downstream, and manoeuvring, which take 59, 31, and 10 % time of the total operational profile, respectively.

Besides the operational profile measurements, the logbook of the ship is used in this study to analyse the transport efficiency. The logbook contains the records of the total amount of cargo transported and total fuel consumed for each journey.

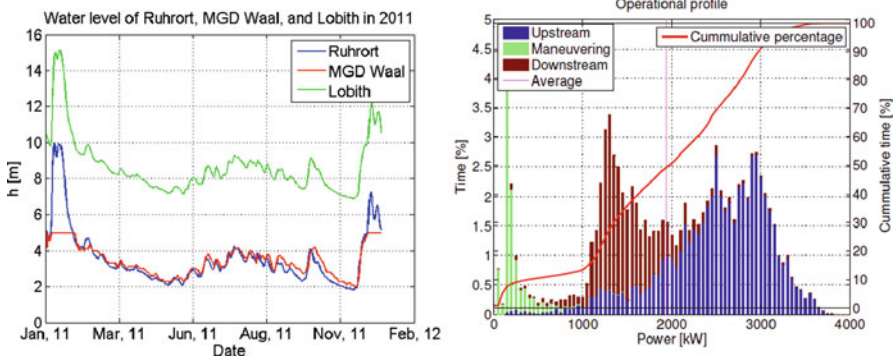


Fig. 20.4 Rhine water levels (left), and operational profile of Veerhaven X during 6 months (right)

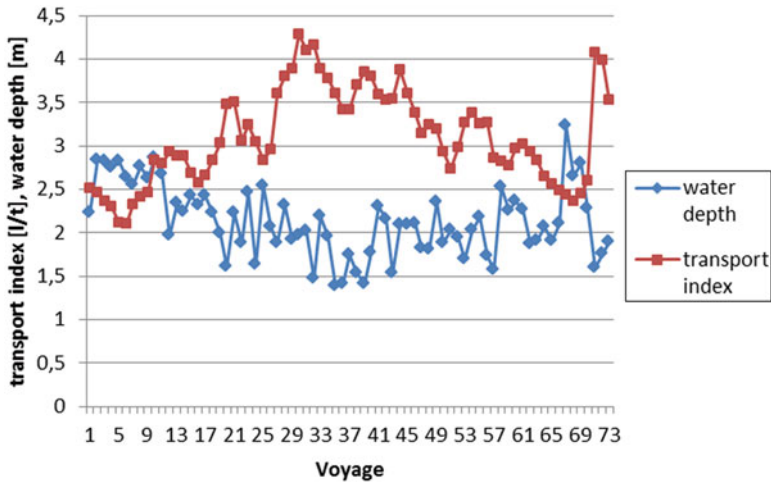
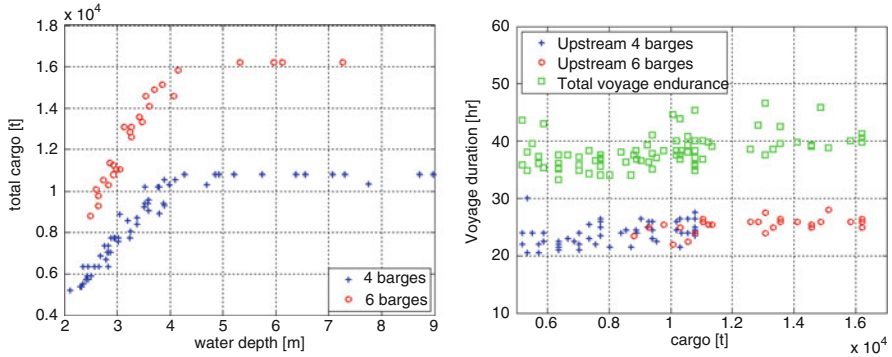


Fig. 20.5 A comparison of the recorded fuel consumptions and cargo transported (l/t) with the water level at river Rhine during 73 voyages of Veerhaven X

By cross-referencing the logbook data with the recorded water levels it is possible to get a link between the water level and transport efficiency. Figure 20.5 shows the transport efficiency together with the recorded water levels, in which the transport efficiency is given as the transport index in terms of the liters of fuel consumed per ton of cargo transported (l/t). Thus, the low values of l/t indicate low fuel consumption and higher efficiency. From Fig. 20.5, it is noticeable how transport efficiency follows the oscillation in water levels. In fact, the transport efficiency can oscillate by a factor two during the recorded 73 journeys.

Based on the operational profile measurements it is possible to further differentiate between the journeys made in four or six barges configuration. Figure 20.6 shows the amount of cargo transported per voyage, in four and six barges configuration,



**Fig. 20.6** Amount of cargo transported in four and six barges configurations (*left*), and voyage duration (*right*)

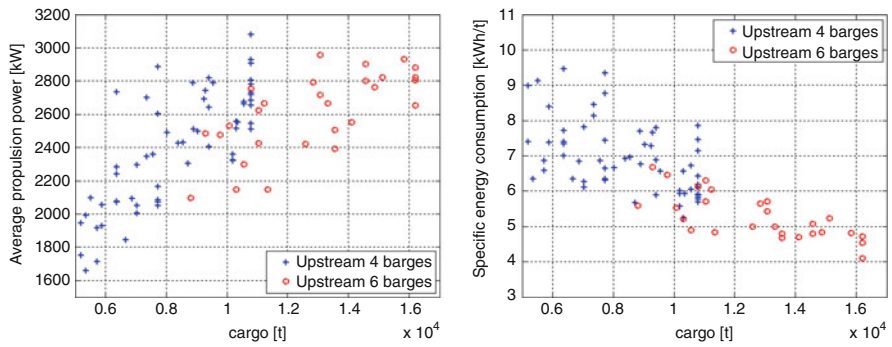


**Fig. 20.7** Average power per journey (*left*) and average specific power (*right*)

and the duration of each voyage. Note that the difference in voyage duration seen in Fig. 20.6 (right) was mostly caused by the waiting time and not by the speed variance.

Further, it is possible to calculate the average power during each voyage. Figure 20.7 shows the average power per voyage and specific average power (kWh/t) per voyage as a function of the cargo transported. In Fig. 20.7, it is noticeable that the voyages with more cargo require less specific average power, i.e., they are more efficient. In previous figures it was shown how the duration of the voyages was more or less constant. Since the distance for each voyage is the same, it is possible to conclude that the speed over ground is similar for all investigated journeys. In fact, the only variable in investigated journeys is the cargo transported. Since water levels dictate the maximal draft of the barges, it is possible to relate the water levels to the cargo transported, i.e., barges are always loaded according to the maximal allowable draft. Subsequently, low water levels will cause low load conditions which will cause an engine to operate in a less efficient region of the operating envelope,

i.e., engine load will be less than 50 % (see Fig. 20.13). Besides this, low water depth may cause an increase in hydrodynamic resistance of the ship due to the shallow water effect, which will deteriorate the transport efficiency even further.

### 20.3 Operational Profile and Transport Efficiency

Besides the operational profile measurements presented in Sect. 20.2, a set of exhaust emission measurements is used in this study as well. The results of the exhaust emission measurements are presented in [8] and they are analyzed in this section. A standard emission measurement test cycle is used (E3 test cycle) to measure the exhaust emissions of the investigated vessel. This is a standard test cycle that applies to propeller law operated main engines and is required by international standards for exhaust emission certification/approval (ISO 8178). Also, legislative requirements are given in weighted cycle average values. As given in Table 20.1, the test cycle consists of four test points where emissions are recorded. For each of the points there is a weight factor and final emission values are weighted average values during the test cycle. Table 20.1 shows the E3 test cycle, with runs at 100, 75, 50, and 25 % of the nominal engine power, and the associated weight factors (WF). In Table 20.1, the engine speed follows from the propeller law and is a function of engine power  $P_B$  relative to nominal engine power  $P_{B0}$  and nominal engine speed  $n_{e0}$ :

$$n_e = n_{e0} \left( \frac{P_B}{P_{B0}} \right)^{1/3}. \quad (20.1)$$

The emission measurements are taken at the steady engine load and the results show average values. The measured emission components are  $O_2$ , CO,  $CO_2$ , NO as  $NO_x$ , HC as  $C_3H_8$ , and PM. The emission measurements are given for the dry exhaust which means that the emission measurements represent the values of a fully dried sample. The exhaust emissions are measured in ppmv and  $mg/m^3$  values. Since legislative limitations are related to the specific power, it is necessary to convert the measurements to kg/h and g/kWh values. The original report in [8] gives emission values in terms of g/kWh as well, but it does not explain the conversion method. The conversion of exhaust emissions from ppmv to g/kWh is explained in [10] and it is named as NLDA method in [5]. Table 20.2 shows weighted cycle average values of Veerhaven X according to the methods described in [8] and [10], respectively named as SGS and NLDA calculation method. As can be seen,

**Table 20.1** E3 emission measurement test cycle

Run	1	2	3	4
rpm	100 %	91 %	80 %	63 %
Power	100 %	75 %	50 %	25 %
WF	0.2	0.5	0.15	0.15



**Table 20.2** Weighted cycle averages of SGS method, NLDA method, and CCNR2 emission regulations

Emission	SGS	NLDA	CCNR2
CO [g/kWh]	0.51	0.54	3.5
HC [g/kWh]	0.78	0.78	1.0
SO <sub>2</sub> [g/kWh]	0.64	0.67	–
NO <sub>x</sub> [g/kWh]	8.03	8.48	8.5
PM	0.08	0.09	0.2

**Table 20.3** Specific fuel consumption versus engine power for SGS, NLDA, and test bed records

Engine power [kW]	263	591	922	1226
sfc SGS and NLDA [g/kWh]	229	202	196	196
sfc test bed records [g/kWh]	239	208	198	196
Difference [%]	4.2	2.9	1.1	0

the emission values from both methods are comparable. Table 20.2 also gives an overview of the allowable exhaust emissions on Rhine as defined by the Central Commission for the Navigation on Rhine (CCNR2) from which it follows that the emissions of Veerhaven X are within the allowed limits.

Regarding the specific fuel consumption (sfc), the manufacturer gives the sfc values for four working points. Table 20.3 shows a comparison of the sfc values measured by SGS and by the manufacturer. For more details regarding the exhaust emission formation and related fuel consumptions the reader can take a look into [10] and [9].

Results shown in Table 20.3 indicate low discrepancy between the specific fuel consumption presented in [8] and the specific fuel consumption measured by the manufacturer. Since the results from Tables 20.2 and 20.3 are used in Sect. 20.5 to calibrate the dynamic models of different power configurations, it is beneficial that the results are cross checked with the manufacturer data. Furthermore, in Table 20.2 it can be observed that the NLDA conversion method is in line with the results presented in [8].

## 20.4 Operational Profile and Transport Efficiency

While in previous sections contain information about the operational profile of Veerhaven X, the goal of this section is to define the alternative power configurations which will be dynamically modelled in order to estimate their total emissions and efficiencies. The alternative configurations will be defined according to the operational profile of Veerhaven X and they include different types of fuel, power arrangement, and transmission options. Regarding the fuel types, alternative configurations will investigate engines which use diesel fuel and natural gas. Regarding the power arrangements, alternative configurations will investigate power configurations with different engine sizes and number of engines, for example



2 smaller engines versus one large engine. Regarding the transmission options, alternative configurations will include the diesel-direct, diesel-electric, and hybrid (i.e., a combination of diesel direct and diesel electric) power transmission.

### 20.4.1 Benchmark Power Configuration

Before defining the alternative power configurations, the benchmark power configuration will be defined first. The benchmark power configuration is based on the power configuration of Veerhaven X but with somewhat altered maximum power. The total power of the benchmark configuration is based on the operational profile shown in Fig. 20.4, where it is noticeable that the maximum recorded total power at the shafts never exceeds 3,800 kW. Also, the recorded auxiliary power never exceeds 250 kW. In order to optimize the benchmark configuration, the benchmark power configuration will have 3,800 kW maximum power delivered at three propeller shafts, and the maximal auxiliary power 250 kW.

### 20.4.2 Alternative Power Configurations

Because of varying water levels, it is argued that a configuration with four propellers might be more beneficial for the pusher. For draught conditions, it is estimated that the efficiency of four propellers, with a smaller diameter, would be much higher than the efficiency of three propellers with a larger diameter. The hydrodynamic performance of the configuration with four propellers was investigated in [2] and it was decided that all alternative power configurations will have four propellers. Figure 20.8 shows the aft ship arrangement for all alternative power configurations where propeller diameter is 1.80 m.

In order to make a fair comparison amongst different power configurations, it is necessary to ensure that the total power delivered to the shaft is the same for all power configurations. Since diesel electric and gas electric power configurations include additional conversions of energy and additional components, the total installed power for these configurations will be larger in comparison with the diesel direct configuration. Figure 20.9 shows an example of a diesel electric power configuration with undefined number of engines and their sizes. The exact number of engines will be defined later.

For electric configurations, the power delivered to the propeller  $P_p$  is a function of the total engine brake power  $P_B$  and the efficiencies of the components between the diesel engine and the propeller:

$$P_p = P_B \cdot \eta_{gen} \cdot \eta_{sw} \cdot \eta_{TF} \cdot \eta_{FC} \cdot \eta_{EM} \cdot \eta_{TRM}, \quad (20.2)$$



Fig. 20.8 Aft ship arrangement of alternative power configurations

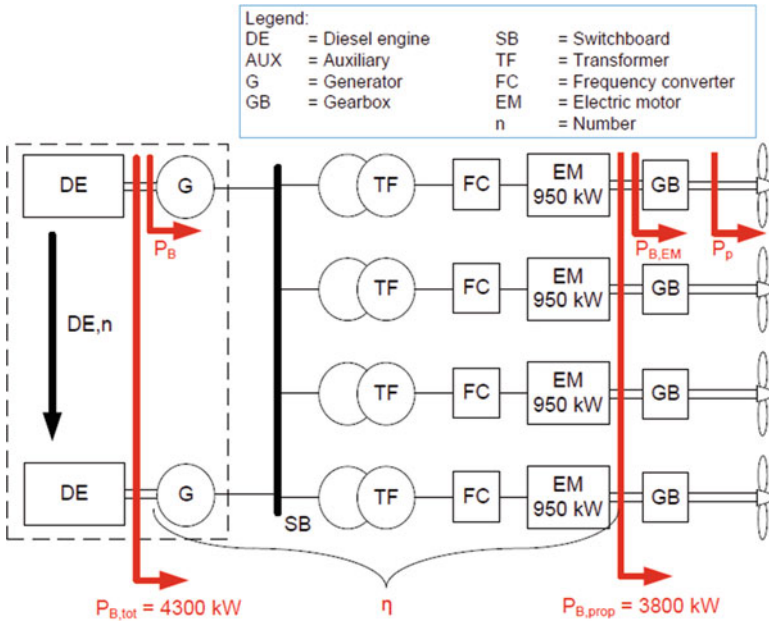


Fig. 20.9 General illustration of diesel-electric power configurations

**Table 20.4** Total installed power for: diesel-direct propulsion (DDP), diesel-electric propulsion (DEP), gas-electric propulsion (GEP), hybrid propulsion (HP), and benchmark power configuration

Power [kW]	DDP	DEP/GEP	HP	Benchmark
$P_{B,max,tot,prop}$	3,800	4,175	3,800 to 4,175	3,800
$P_{B,max,tot,aux}$	2*125	125	2*125 to 125	2*125
$P_{B,max,tot}$	4,050	4,300	4,050 to 4,300	40,500

where the efficiencies of the components are defined as:

- Generator efficiency  $\eta_{gen} = 0.97$  and electric motor efficiency  $\eta_{EM} = 0.97$  as in [6]
- Switchboard efficiency  $\eta_{SW} = 0.999$ , transformer efficiency  $\eta_{TF} = 0.997$ , and frequency converter efficiency  $\eta_{FC} = 0.97$  as in [1]

In general, electrical power configurations are more suitable for ships with high auxiliary power demands, for example see [3], because of their flexibility of power generation and distribution. As a consequence they need smaller auxiliary engines, and therefore it will be assumed that only one half of the total auxiliary power is needed for the alternative electric power configurations. The other half will be added to the total power installed ( $P_{B,tot}$ ). Table 20.4 shows the summary of the total maximum installed power for different power configurations.

Since power configurations which use natural gas currently run only in electric power configuration, the total installed power for gas-electric power configurations (GEP) will be the same as for the diesel-electric power configurations (DEP). The hybrid power configuration (HP) will be a combination of diesel-direct and diesel-electric power configuration, and the total installed power for hybrid power configurations could be between the total power needed for diesel-direct power configurations and the total power needed for diesel-electric power configurations. Table 20.5 shows possible alternative configurations with diesel-direct (DDP), DEP and GEP, and HP. In the table, the candidates are given for a combination of maximum engine brake power. The number of different engine sizes ranges from one to three different sizes and the total number of engines installed ranges from one to five engines. In the columns, the number before the asterisk sign, “\*”, is the number of engines and the number after the asterisk sign is the maximum engine brake power in kW.

### 20.4.3 Selection of Alternative Power Configurations

The selection of the alternative configurations from the candidate alternatives is based on:

**Table 20.5** Candidate alternative configurations

Nr. of engine sizes	Nr. of engines	DDP [kW]	DEP/GEP [kW]	HP [kW]	
				DDP	DEP
1	1	3,800	4,300	–	–
	2	1,900	2,150	2,050	2,050
	3	1,267	1,433	1,380	2*1,380
	4	950	1,075	2*1,020	2*1,020
	5	–	860	2*825	3*825
2	2	3,000+800	1,800+2,500	1,900	2,200
	3	2*950+1,900	2*800+2,700	1,900	2*1,100
	4	2*800+2*1,100	3*800+1,900	2*950	2*1,100
	5	–	4*800+1,100	2*800	3*850
3	3	2,000+1,000+800	2,500+1,000+800	1,900	1,900+1,800
	4	800+900+2*1,050	800+1,000+2*1,250	2*950	900+1,300

- The time percentage that engines run in the optimal fuel consumption region throughout the operational profile.
- Equal load share is assumed amongst the engines.

The optimal fuel consumption region was assumed to be between 50 and 85 % of engine power and Table 20.6 presents the calculated time fractions of the candidate configurations and the power configurations which are selected for further investigation (marked with bold letters). Even though power configurations with three different engine sizes have high time percentage of optimal fuel consumption, it was decided not to include them into further consideration because of the related spare parts and maintenance aspects.

Based on the results shown in Table 20.6, the following power configurations are selected for further investigation:

- Benchmark configuration: diesel-direct power configuration with three shaft lines and three 1,267 kW engines
- DDP 4\*950: alternative diesel-direct power configuration with four shaft lines and four 950 kW engines
- DDP 2\*950 + 1,900: alternative diesel-direct power configuration with four shaft lines, two 950 kW engines, and one 1,900 kW engine. The larger engine is driving two propellers, and each smaller engine is driving separate propeller.
- DDP 2\*800 + 2\*1,100: alternative diesel-direct power configuration with four shaft lines, two 800 kW engines, and two 1,100 kW engines. This configuration consists of two father-son drives, where each father-son drive consists of one 800 kW engine, one 1,100 kW engine, father-son gearbox, and two propellers.
- DEP/GEP 5\*860: alternative diesel-electric or gas-electric power configuration consisting of five 860 kW generator sets and four shaft lines.

**Table 20.6** Cover coefficient of candidate configurations where the selected alternative configurations are bolded

Nr. of engine sizes	Nr. of engines	DDP		DEP/GEP		HP [kW]		t [%]
		Power [kW]	t [%]	Power [kW]	t [%]	DDP [kW]	DEP [kW]	
1	1	38,00	55	4,300	57	-	-	-
	2	1,900	83	2,150	83	2,050	2,050	86
	3	<b>1,267</b>	<b>85</b>	1,433	89	1,380	2*1,380	89
	4	<b>950</b>	<b>94</b>	1,075	94	2*1,020	2*1,020	94
	5	-	-	<b>860</b>	<b>95</b>	2*825	3*825	94
2	2	3,000+800	71	1,800+2,500	94	1,900	2,200	93
	3	<b>2*950+1,900</b>	<b>94</b>	2*800+2,700	94	1,900	2*1,100	94
	4	<b>2*800+2*1,100</b>	<b>95</b>	<b>3*800+1,900</b>	<b>94</b>	2*950	2*1,100	94
	5	-	-	<b>4*800+1,100</b>	<b>95</b>	<b>2*800</b>	<b>3*850</b>	<b>95</b>
3	3	2,000+1,000+800	94	2,500+1,000+800	95	1,900	1,900+1,800	95
	4	800+900+2*1,050	94	800+1,000+2*1,250	95	2*950	900+1,300	95

- DEP/GEP 3\*800 + 1,900: alternative diesel-electric, or gas-electric power configuration consisting of three 800 kW generator sets, one 1,900 kW generator set, and four shaft lines.
- DEP/GEP 4\*800 + 1,100: alternative diesel-electric, or gas-electric power configuration consisting of four 800 kW generator sets, one 1,100 kW generator set, and four shaft lines.
- HP DDP2\*800+DEP3\*850: alternative hybrid power configuration with two 860 kW diesel engines driving two propellers, and three (diesel) generator sets of 850 kW driving the other two propellers.

### 20.5 Dynamic Models

This section describes the dynamic models of the selected power configurations from Table 20.6 in the previous section. The block diagram of the models used in this study is in Fig. 20.10 and it shows the structure of the models. The model in Fig. 20.10 is developed in MatLab/Simulink environment and it will be used to estimate the related emissions ( $em_{prop,j}$ ) and fuel consumptions ( $fc_{prop}$ ). The inputs to the model are the operational profile measurements ( $P_{prop,up}$ ) and cargo loaded ( $\nabla_{tot,loaded}$ ). Instead of immediately trying to trace back the measured operational profile to the fuel consumed, an attempt is made to have a realistic simulation of the

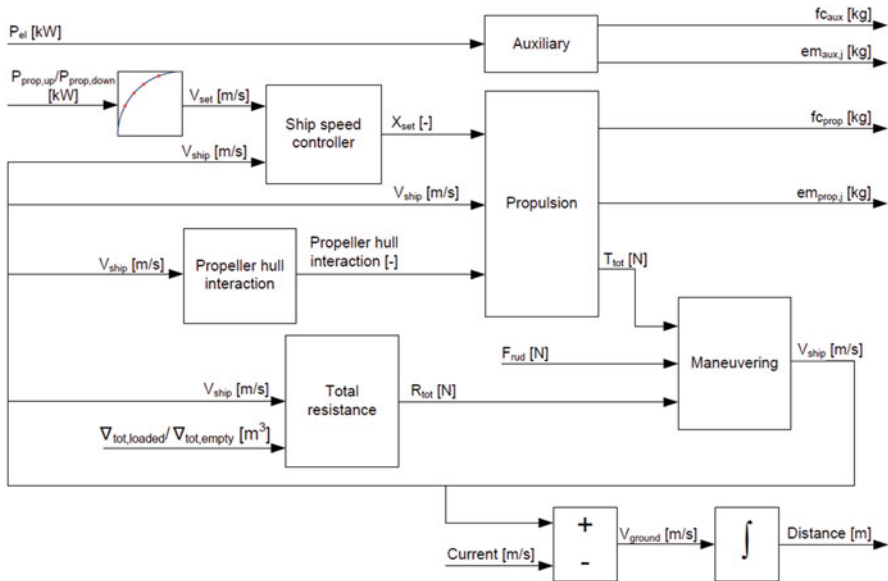
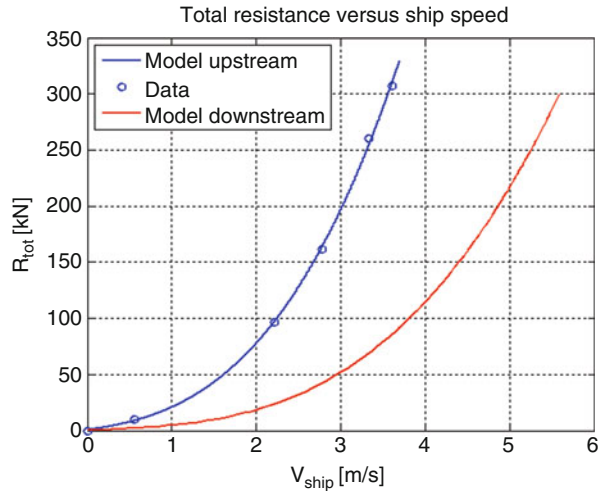


Fig. 20.10 Block diagram of dynamic model used in this investigation

**Fig. 20.11** Modelled resistance in upstream and downstream mode, and measurement data as in [2]



voyage with the ship speed controller block imitating the helmsman. In the model, the measured power is converted to the set speed ( $V_{set}$ ), using the ship resistance curve, which is then converted to the fuel rack setting ( $X_{set}$ ). Figure 20.11 presents the total resistance of the model in upstream (loaded condition) and downstream mode (empty condition) according to the data provided in [2]. Also, coefficients for the propeller-hull interaction were derived from [2]. In Fig. 20.10, the manoeuvring block has the possibility to include the manoeuvring forces in the rudder to fully simulate the voyage trajectory. The manoeuvring forces are modelled according to [7]. However, the applicability and accuracy of Kijima model for the case of Veerhaven X is not known. Thus, in order to reduce the uncertainties and speed up the computation time, the manoeuvring possibility is switched off and the model assumes a straight line trajectory.

Perhaps the most elaborate part of the model is the propulsion block in Fig. 20.10. The purpose of the propulsion block is to calculate the thrust based on the fuel rack setting. Figure 20.12 shows the structure of the propulsion block. Depending on the specific power configuration, the engine block will contain the diesel and/or the gas engine models. The diesel engine model uses the Seiliger cycle and it is described in [11]. The gas engines are modeled with the “Mossel” engine model which is described in [11] and [10].

Figures 20.13 and 20.14 show matching of fuel consumption characteristics of the modelled diesel and gas engines with the available data for four different engines: two diesel engines and two spark-ignition gas engines. Namely:

- 1,360 kW diesel engine in Fig. 20.13 left was used to match the models of 800, 850, 860, 900, 1,100, and 1,267 kW diesel engines
- 1,900 kW diesel engine in Fig. 20.13 right was used to match the models of 1,900 kW diesel engine
- 1,000 kW and 1,900 kW gas engine in Fig. 20.14 was used to match the models of 800, 860, 1,100, and 1,900 kW gas engines



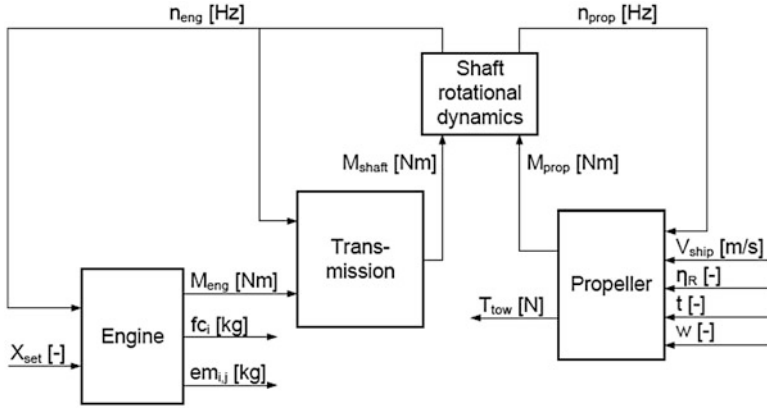


Fig. 20.12 Block diagram of Propulsion block in Fig. 20.10

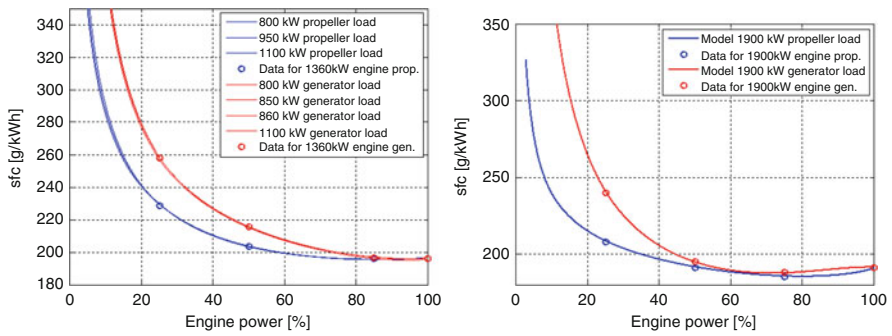
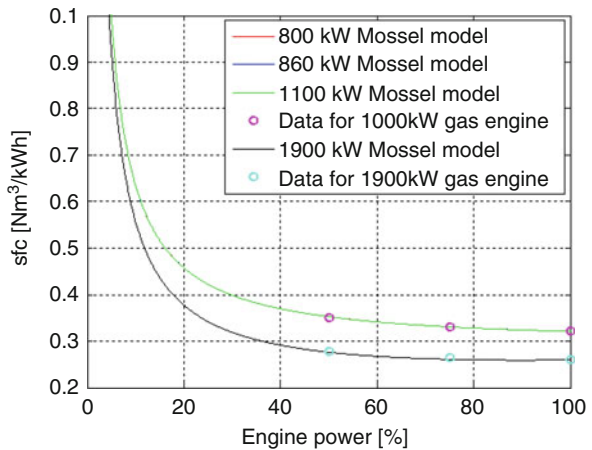


Fig. 20.13 Matching of specific fuel consumptions with the test bed records of 1,360 kW diesel engine (left) and 1,900 kW diesel engine (right)

Fig. 20.14 Matching of specific fuel consumptions with the test bed records of 1,000 and 1,900 kW gas engine



The power transmission block shown in Fig. 20.12 will be different for diesel-direct power configurations and for diesel/gas-electric power configurations. For diesel-direct power configurations the transmission block is a gearbox with the constant gearbox ratio. Only for “DDP 2\*800 + 2\*1,100?” the gearbox will have the father-son gearbox ratios. For electric power configurations, the transmission block consists of switchboards, frequency converters, and electric motors. The model for electric motors is based on the wound rotor model presented in [4]. For all power configurations some power management system is needed to regulate the number of engines switched on and their loading distribution. The exact rules used to control the number of running engines are based on the operational profile of one typical journey which is presented in the next section.

## 20.6 Modeled Results

The aforementioned dynamic models are used to calculate the emissions of the alternative power configurations during one typical journey between Rotterdam and Duisburg. Figure 20.15 shows the propulsion power in kW versus voyage duration in %, during the investigated journey. In the model, the total voyage duration is: 24 h upstream, and 13 h downstream. The current is set to 0 m/s in Rotterdam and 1.66 m/s in Duisburg with linear increase during the voyage. The current is negative when sailing from Rotterdam to Duisburg and positive when sailing from Duisburg to Rotterdam. The total cargo transported in the loaded condition is 14,700 tons which is based on the logbook of Veerhaven X.

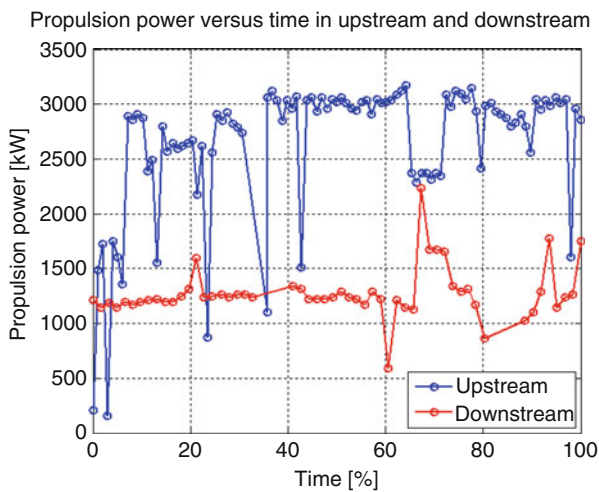


Fig. 20.15 Input propulsion power in upstream and downstream mode of one typical voyage

As mentioned in the previous section, for each configuration it is necessary to decide on the number of engines that are running and the load share amongst the engines. Because of uncertainties related to the performance of the propellers in the trailing shaft conditions, it was assumed that all propellers are always running in both operation modes (upstream and downstream mode). This assumption is also supported from every-day sailing practice. For most of the diesel-direct power configurations this will mean that all engines are always on (for both operation modes). Only for the father-son power configuration (DDP 2\*800 + 2\*1,100) it is possible to switch off some engines in the downstream mode. For diesel-electric and gas-electric power configurations, especially in the downstream mode, it is not necessary that all engines are always running on. This is especially beneficial for electric configurations with the 1,900 kW engine where the priority was given to the larger engine because of their higher efficiencies. Regarding the number of engines running, general rule is to have engines running between 50 and 85 % of their maximum power (as defined in Figs. 20.13 and 20.14). Regarding the load sharing, equal load share amongst the running engines was assumed for all power configurations, except for the GEP 3\*800+1,900 for which the larger engine is more loaded due to its significantly higher efficiency.

Since diesel and natural gas fuel have different lower heating values (LHV), the resulting fuel consumption is represented as the resulting energy consumption. The total energy consumption was the sum of all individual consumptions for each power configuration during the investigated voyage. The energy consumption per engine was calculated according to:

$$E = LHV \cdot \int_{t_{begin}}^{t_{end}} \dot{m}_f dt, \tag{20.3}$$

where  $\dot{m}_f$  is the fuel flow. For diesel fuel the LHV for diesel is 42.7 and LHV for gas (LNG) is 43.64 was assumed. Figures 20.16 and 20.17 show the resulting energy

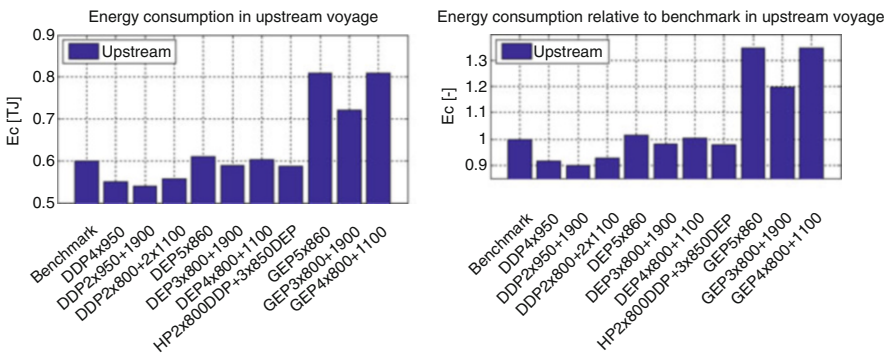


**Fig. 20.16** Comparison of energy consumption of Benchmark, diesel-direct, diesel-electric, gas-electric, and hybrid power configurations for upstream part of the voyage

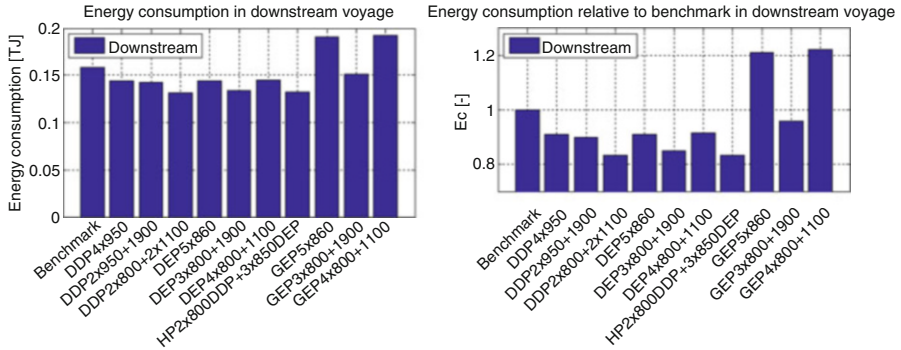


**Fig. 20.17** Comparison of energy consumption of Benchmark, diesel-direct, diesel-electric, gas-electric, and hybrid power configurations for downstream part of the voyage

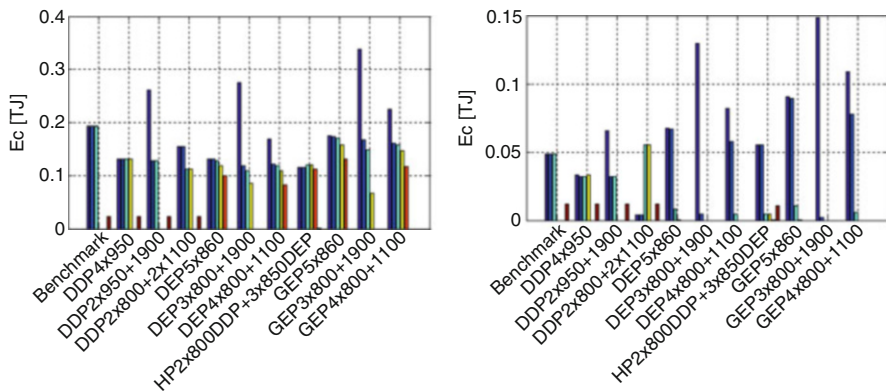


**Fig. 20.18** Energy consumption per engine in upstream (*left*) and downstream part of the voyage (*right*)

consumptions of all power configurations for the upstream and downstream part of the investigated journey. Figure 20.18 shows energy consumptions of each engine for all power configurations for the upstream and downstream conditions. Bars in the graphs show energy consumption of each engine in the configuration, where the largest engine is the first bar. For example in DEP 3\*800+1,900, first bar is the engine of 1,900 kW and the other three bars are 800 kW.

Figure 20.19 shows the total energy consumption of the entire journey for all power configuration and Fig. 20.20 shows the total emissions of all diesel-direct and diesel-electric power configurations for the entire journey. The figure shows the total emissions of all engines per power configuration. Emissions of gas-electric power configurations are presented separately in Fig. 20.21. The results of the models are discussed in the next section of this chapter.

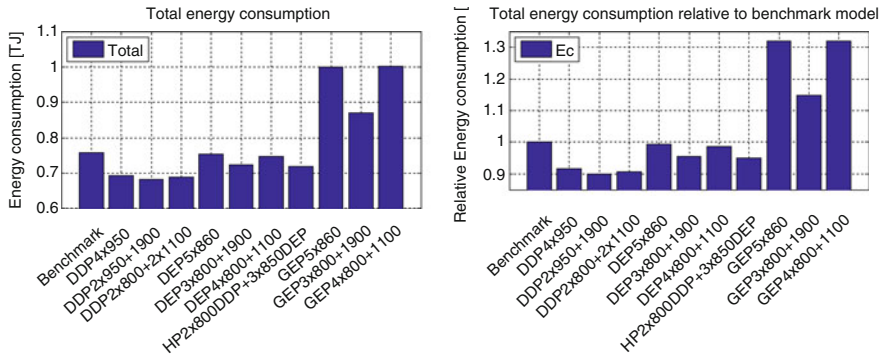


**Fig. 20.19** Comparison of energy consumption of Benchmark, diesel-direct, diesel-electric, gas-electric, and hybrid power configurations for the entire voyage

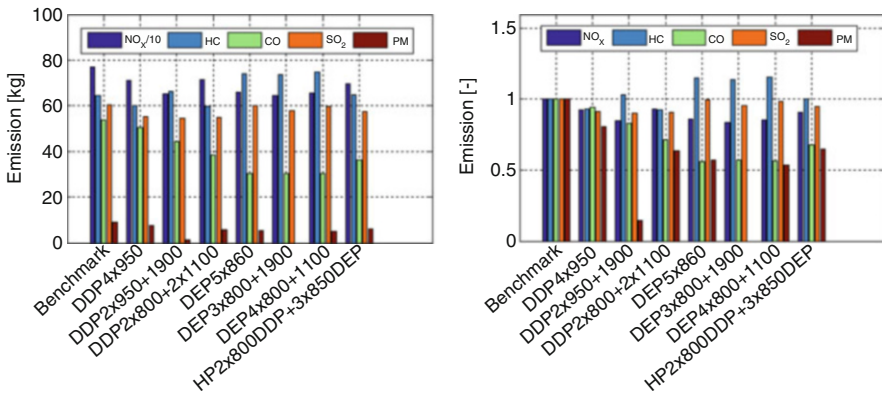


**Fig. 20.20** Resulting emissions of diesel-direct and diesel electric power configurations for the investigated voyage

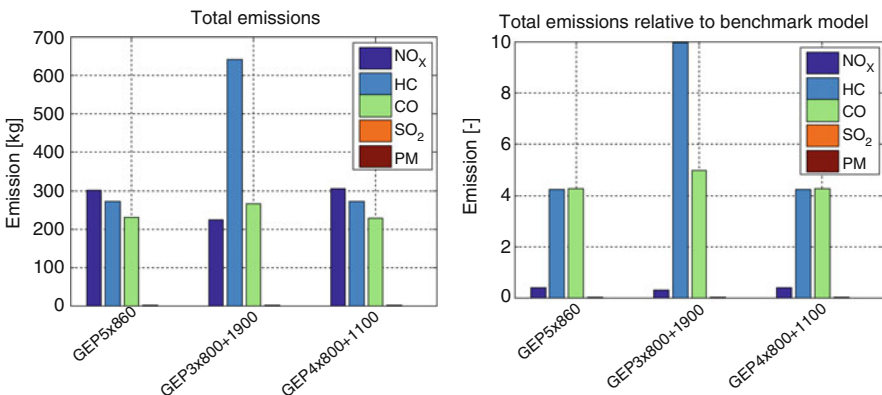


**Fig. 20.21** Total emissions of configurations with gas engines (*left*) and their emissions relative to the emissions of the benchmark configuration (*right*)

## 20.7 Discussion

Before discussing the results of the analysis given in Sect. 20.6, it is useful to compare some of the results with the logbook records of the ship. For the investigated journey, it was recorded that the amount of fuel consumed was 21 ton of diesel while the benchmark model in Fig. 20.19 gives an estimate of 18 tons of diesel. It should be mentioned that the logbook shows the consumptions between 19 and 24 tons for journeys with similar cargos. Since the benchmark model has somewhat smaller and more efficient engines than the real ship, the estimate of the benchmark model seems realistic. Moreover, the correctness of the model has been evaluated against the emissions and fuel consumption measurements.

The difference amongst the fuel consumptions recorded in the logbook results partially from the difference in water levels. A low water level can influence the performance of the ship in several ways: it limits the draft of the barges and the cargo loaded, it increases the resistance due to the shallow water effect, and the propellers might not be fully submerged. Since water levels can vary between 2 and 10 m, it was decided that all alternative configurations have four propellers instead of three. Even though the analysis shows that the alternative configurations have higher efficiency than the benchmark model, it should be noted the effect of low water levels was not fully investigated here. The best way to evaluate the performance of all configurations would be to calculate the related fuel consumptions for the entire operational profile during 1 year. Since this data is not available, and the data related to the performance of the three-shaft configuration in partially submerged conditions is also not available, it was decided to leave this analysis for future work. Nevertheless, the work done in this chapter shows that it is possible to get 10 % improvement in the efficiency just by selecting another power configuration.

Looking at the investigated configurations, the DDP 2\*950+1,900 seems to be the most efficient power configuration. Also the total amount of exhaust emissions is favorable with this configuration. There are probably few reasons for this, one is high time percentage of the optimal engine usage presented in Table 20.6 and another reason is better engine efficiency for 1,900 kW diesel engine, presented in Fig. 20.13. Also, the diesel-direct power configurations have advantage over the electric power configurations because of less components and one energy conversion less. However, the diesel-electric power configurations show quite respectable performance, in general even better than the benchmark model. Looking at the gas engine configurations they provide large  $\text{NO}_x$  reduction but their total energy consumption is higher than for DDP. This is explained by lower combustion efficiency of gas engines, which is expected to be improved in the coming years. Other benefit of gas engines is that they produce less  $\text{CO}_2$  in comparison with diesel engines. However, their production of hydrocarbon gasses and carbon monoxide is not favorable in comparison with diesel engines. Again, the gas configuration with the large 1,900 kW engine shows best results amongst gas engine configurations. Here it should be mentioned that further improvement of the results could be achieved for all power configurations if the trailing propeller mode was allowed.

This would improve their performance mainly in the downstream mode. It is estimated that the overall improvement of the efficiency would be around 1 % due to trailing propellers.

## 20.8 Conclusions and Future Work

The goal of this chapter was to investigate the performance of alternative power configurations of an inland pusher on river Rhine. As in many other performance analysis, this analysis is driven by two motivations. First motivation was an economical motivation, i.e., an attempt was made to estimate the fuel consumption of different power configurations. The second motivation was a legislative motivation, i.e., an attempt was made to estimate which configuration agrees with the current and future exhaust gas limitations. Looking at the current exhaust gas limitations, all investigated power configurations fall below the current exhaust gas limitations set by CCNR. However, it is expected that the future limit for  $\text{NO}_x$  emissions will be set to 1.8 g/kWh. While for gas engines this limit is ok, for diesel engines the forecasted  $\text{NO}_x$  limit will be challenging. An option for diesel engine power configurations is to add a selective catalytic reduction (SCR) device which reduces the  $\text{NO}_x$  emissions. Since SCRs use urea to operate, it is convenient to know how much urea is needed for a modern diesel engine to meet the future  $\text{NO}_x$  limit. Looking at the equation presented in [12] it is possible to estimate that a ship such as Veerhaven X would use around 15l of urea per MWh. Based on its performance, an SCR installation seems to be a practical solution for retrofitting of older vessels.

Based on the results for one representative journey, the diesel direct power configuration seems to be the most efficient. However, the gas-electric configurations are superior regarding the  $\text{NO}_x$  emissions. Even though the analysis done above used one specific vessel for the case study, it is possible to draw some general conclusions. Based on the entire analysis, it is possible to conclude that the gas engines (or dual fuel engines) have a lot of potential and probably will be more used in the future. On the other hand, modern diesel engines are still good option for new build vessels and definitely very good option for retrofit of old vessels. In combination with an SCR it is conceivable that diesel engines will remain the main prime movers of inland vessels for coming years. As shown in this chapter, the transport over inland waterways is closely related to the water level. By transporting the water it should be possible to increase the water depth on an inland waterway and increase the transport efficiency during the periods of low water levels. However, the feasibility of this proposal remains to be scrutinized in the future.

**Acknowledgements** This research has been partially supported by EU-FET granted project: “Modernisation of Vessels for Inland waterway freight Transport MOVE IT!”, project reference number: 285405. Authors would like to thank ThyssenKrupp Veerhaven B.V., in particular Mr. Be Boneschansker for his support.



## References

1. Adnanes AK. Maritime electrical installations and diesel electric propulsion. ABB, 2003.
2. Bieker K. Future pusher bericht 2072. Internal report, technical report, DST - Development Centre for Ship Technology and Transport Systems, 2012.
3. Buckingham J. Hybrid drives for naval auxiliary vessels. Technical report, Engineers Australia, 2013.
4. de Ryuck K. Simulation of advanced engine room configurations with energy savings concepts. MSc thesis, report nr.: Sdpo.11.020, TU Delft, 2011.
5. Drijver M. Future pusher project. MSc thesis, report nr.:SDPO.13.030, TU Delft, 2013.
6. Frouws JW. Aes decision model. Technical report, TU Delft, 2008.
7. Kijima K, Nakiri Y, Katsuno T, Furukawa Y. On the manoeuvring performance of a ship with the parameter of loading condition. *J Soc Nav Archit Jpn.* 1990;168:141–8.
8. SGS. Resultaten emissiemetingen van de motoren van duwboten. Internal report, technical report, SGS Nederland B.V., 2010.
9. Shi W. Dynamics of energy system behaviour and emissions of trailing suction hopper dredgers. PhD thesis, TU Delft, 2013.
10. Stapersma D. Diesel engines volume 4: Emission and heat transfer. Lecture notes, TU Delft, 2010.
11. van Deursen EW. Control of hybrid ship drive systems. MSc thesis, report nr.:SDPO.11.022, TU Delft, 2011.
12. Wartsila. Imo tier III solutions for Wartsila 2-stroke engines – selective catalytic reduction (scr). Product brochure, Wartsila, 2011.